

ANALYTICAL STUDY ON RELIABILITY OF SEISMIC SITE-SPECIFIC CHARACTERISTICS ESTIMATED FROM MICROTREMOR MEASUREMENTS

Boming ZHAO¹, Masanori HORIKE² And Yoshihiro TAKEUCHI³

SUMMARY

We have examined the site specific ground characteristics estimated by microtremor measurements and earthquake observation at the arrays set up in Kushiro district, Japan. It suggested from these examinations that the microtremor measurements are usable as an effective tool to estimate the seismic site-specific characteristics of ground. In this paper, we examine a reliability of the microtremor measurements as a tool of estimating site-specific characteristics by comparing the estimation results at the arrays in the Kushiro and at another arrays in Kansai district. These arrays located in different geological conditions. Further more, we discuss a propagation characteristics of microtremors in specific ground model by numerical simulation based on hybrid method of BEM and TLFEM.

INTRODUCTION

Microtremors have been proposed as simple and effective tools to estimate ground response characteristics in site [e.g., Kanai *et al.*, 1954; Irikura and Kawanaka, 1980]. However, these proposals not be summarized in to their theoretical background and applicable conditions as yet. In order to save these problems, we have been compared estimation results of microtremors and seismic motions from array observation [Zhao *et al.*, 1996; Zhao *et al.*, 1997; Zhao *et al.*, 1998a; Zhao *et al.*, 1998b]. In this paper, we discuss a reliability of seismic site-specific characteristics estimated from microtremor measurements by comparing the results from Kushiro and Kansai district, Japan, located under different conditions with respect to geological structure and microtremor source effect. Further more, to explain these observational conclusions, we calculate and compare the site-specific ground characteristics from surface wave of microtremors and seismic wave simulated by two 2D laterally heterogeneous multi-layered models theoretically, the modeling is based the ground conditions of Kushiro district in east-west direction. Surface waves and seismic waves are defined as surface point sources and plane P-SV-wave incidence, respectively. Numerical simulations are computed by using hybrid method of the boundary element method (BEM) and the thin layer finite element method (TLFEM).

In this study, we use three site-specific characteristics to discuss above-mentioned purposes. The characteristics consist of specifically the predominant frequency, the spectral ratios of horizontal components between different sites (hereafter HH spectral ratio), and the spectral ratio of horizontal to vertical component ratio (hereafter HV spectral ratio) .

2 EXPERIMENTAL STUDY

2.1 Array observation procedures

Two difficult observation networks located in Kushiro and Kansai district are chosen as the observation areas in this spatial variation study. Figure 1 shown the location of all arrays in the two areas. Kansai district was an area hit by the Great-Hansin Earthquake ($M_J=7.3$) and Kushiro district is chosen partly because the area showed remarkable spatial variation of quake damages in 1993's Oki-Kushiro Earthquake ($M_J=7.1$).

¹ Geo-Research Institute, Osaka, Japan. zhao@geor.or.jp

² Osaka Institute of Technology, Osaka, Japan. hrk1@archi.oit.ac.jp and takeuchi@archi.oit.ac.jp

³ Osaka Institute of Technology, Osaka, Japan. hrk1@archi.oit.ac.jp and takeuchi@archi.oit.ac.jp

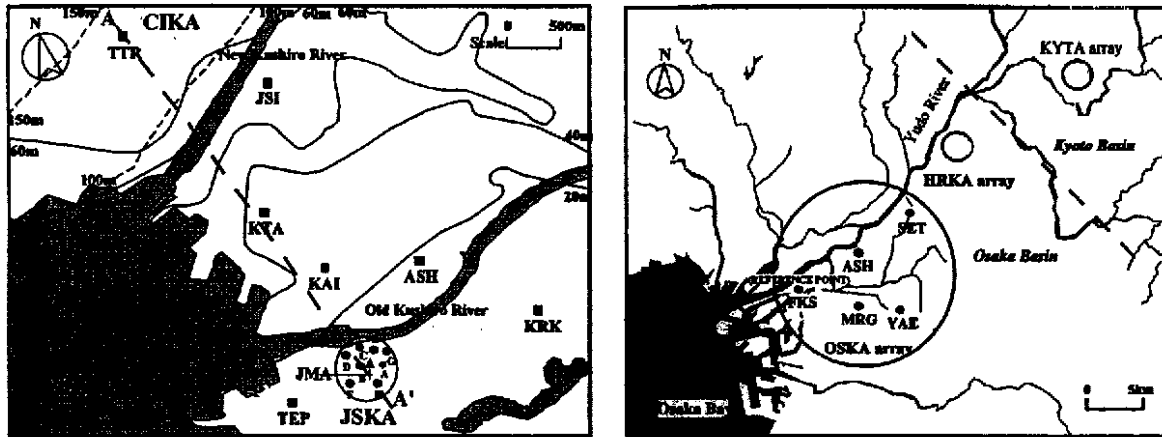


Figure 1. Location of observation points of JSKA-, CIKA-array in Kushiro district (left diagram), OSKA-, HRKA-, KYTA-array in Kansai district (right diagram).

The Kushiro observation network were composed by two arrays (JSKA and CIKA). The JSKA-array locates in the Kushiro plateau. The diameter of the array is about 500 m around Kushiro JMA, and 8 sites were installed on the plateau. The shallow portions of the plateau are composed of soft volcanic ashes, and a hard Tertiary formation lies beneath it. The CIKA-array size approximately 6km×4km. Five site are in the Kushiro alluvium plains west of Kushiro river, and 2 sites are in the Kushiro plateau east of the river. The reason for that two different-size arrays were deployed is to examine to what spatial extent site responses from microtremors are in agreement with those of seismic motions. Three arrays in Kansai observation network that are OSKA-array, KYTA-array and HRKA-array are shown by circle of solid line in Figure 1 (right diagram) The large OSKA-array, the small KYTA- and HRKA-array are formed by five observation sites located on the alluvium layer of Osaka basin, seven observation sites located on the reclaimed land of the south of Kyoto basin, and four observation sites located respectively. The OSKA- and KYTA-array are used to estimate reliability of using microtremor measurements in different areas by comparing the results with Kushiro arrays. The HRKA-array is used to discuss what change are occurred for three characteristics whit other arrays deployed on soft surface ground (e.g., alluvium deposits).

2.2 Predominant frequencies of power spectra and HV spectral ratios

The predominant frequency of sediments has been estimated from microtremors [e.g., Kanai and Tanaka, 1961] for the simplicity of observation and analysis. However, it was often reported that the predominant frequency does not always reflects that of sediments. Therefore we compare predominant frequency estimated from seismic motions with one from the power spectra and from the HV spectral ratios of microtremors. Figure 2 show the typical analysis results as to JSKA-, CIKA-, OSKA- and KYTA-array in which microtremor power spectra (thick line), microtremor HV spectral ratio (bold line) and seismic motion spectra (dotted line). In this Figure, we find that the peak frequencies of seismic motions are observed at almost sites, where those of microtremors are observed either. We define the predominant frequency as the peak frequency which appears in the power spectra of all seismic events, as shown by solid circles, the peak frequencies of microtremors, as shown by crosses. As these site, we found that the peak of mcicrotrmor HV spectral ratios are very conspicuous than the power spectra, and the frequency coincide with those of seismic motions. However, we also found that at some site (e.g., ASH, SET and YAE) microtremor power spectra show peak but their frequencies do not coincide with those of seismic motions exactly. On the other hand, in KAI site the microtremors and seismic motions don't have clear peak in the whole frequency range.

As a result, it follows that observation of microtremor HV spectral ratios are more reliable and more effective than that of microtremor power spectra in estimating predominant frequencies of seismic motions.

2.3 HH spectral ratios between different observation sites

In this section, it is examined whether spatial variation of seismic motions can be estimated by utilizing microtremor power spectral ratios with reference to a standard observation site. The examples of observation results of JSKA-, CIKA- and KYTA-array are indicated from Figure 3. The microtremor measurements obtained form OSKA-array have not simultaneity. In this Figure, two thin lines denote the mean plus the standard

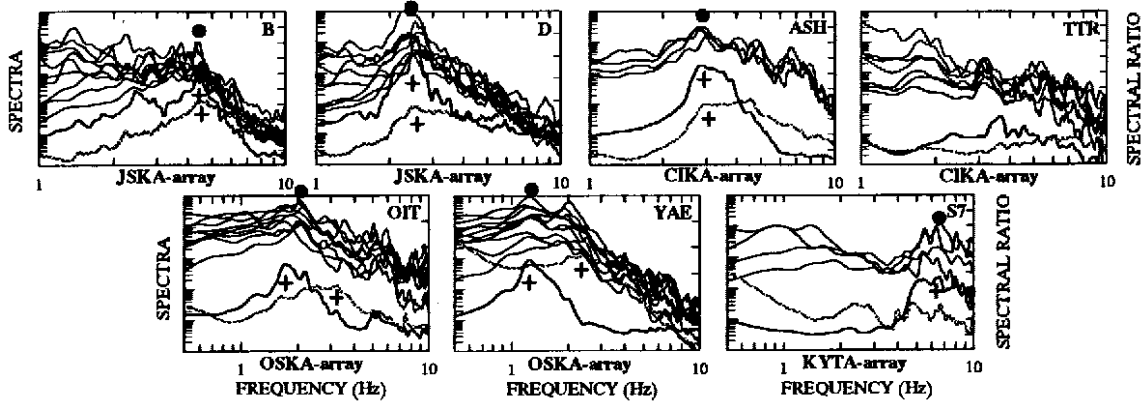


Figure 2. Amplification characteristics among microtremor spectra, microtremor HV spectral ratios and seismic motion spectra at JSKA-, CIKA- (Kushiro), OSKA- and KYTA-array (Kansai).

deviation of seismic motions HH ratios and the mean minus the standard deviation of them, thick lines denote the microtremor HH spectral ratios. An example of the relation of a standard deviation and a scattering of HH spectral ratios is shown as to the B/A (HH) result. In small array JSKA and KYTA, space between two thin lines are narrow and show similar characteristics as to each earthquake event. As for the comparison between the seismic HH ratios and those of microtremors, values of the latter ratios are within limits of standard deviations of the former in the low frequency range concerning all the observation sites whether the spatial variation are shown or not. In large array CIKA, the spectral sharp is similar to each other, but the values are quite different in almost sites.

As mentioned above, microtremor HH spectral ratios almost coincide with those of seismic motions concerning the small arrays, but they differ greatly concerning the large array CIKA. One of the reasons of this great difference might be that spatial distribution of microtremor sources (spatial density of sources and location of them at observation sites) is not uniform within the area of large array, because the spatial distribution of microtremor sources depends on the level of human activities and underground structures on site. These results suggest reliability of estimating the seismic spatial variation by utilizing the microtremor HH ratios, if the frequency range is restricted in small area.

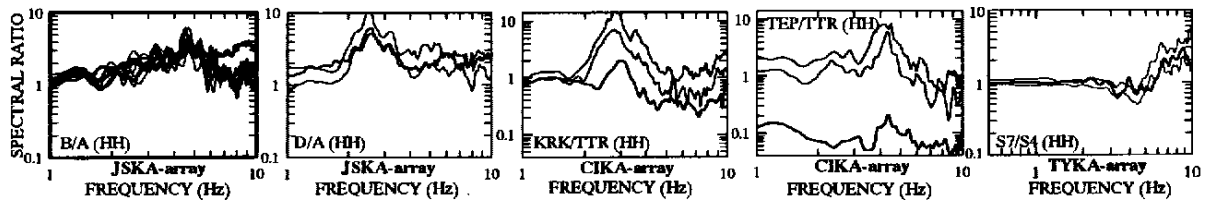


Figure 3. HH spectral ratios among microtremors and seismic motions for JSKA-, CIKA- and KYTA-array.

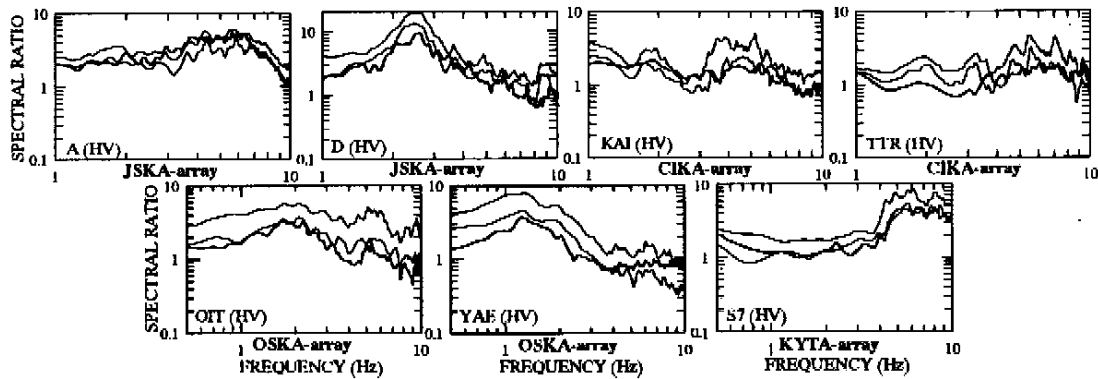


Figure 4. HV spectral ratios among microtremors and seismic motions for JSKA-, CIKA- (in Kushiro), OSKA- and KYTA-array (in Kansai).

2.4 HV spectral ratio

HV spectral ratio can be utilized as a transfer function of estimating vertical component from horizontal one of seismic motions, if HV spectral ratios are supposed to be specific on each observation site. From this viewpoint, HV spectral ratios of microtremors are compared with these of seismic motions. Figure 4 show HV spectral ratios of JSKA-, CIKA-, OSKA- and KYTA-array. Two thin lines denote the mean plus and minus the standard deviation of seismic HV ratios, and thick lines denote microtremor HV ratios. In these arrays, we found that microtremor HV spectral ratios indicate to be same to seismic motions ones or the values are some smaller than that of seismic motions.

These results suggest reliability of estimating the vertical component from the horizontal one of seismic motions using by microtremor HV spectral ratios, if an appropriate corrections are established with respect to the values of microtremor HV spectral ratios.

2.5 Results of the hard surface ground

Figure 5 shows comparison results recorded at HRKA-array which has a diluvial surface layer ($V_s=450\text{m/s}$). In this cases, power spectra of microtremors and seismic motions are clear in almost the same frequency range and show correlation, but the HV spectral ratios of microtremors do not show clearly peak than power spectra. These results are contrary with those from soft surface ground. On the other hand, the HH, HV spectral ratios of microtremors and seismic motions are comparably flat in the all frequency range. As for the comparison between the seismic spectral ratios and those of microtremors, the both spectral ratios are agreement, and result are similar with those from soft surface ground.

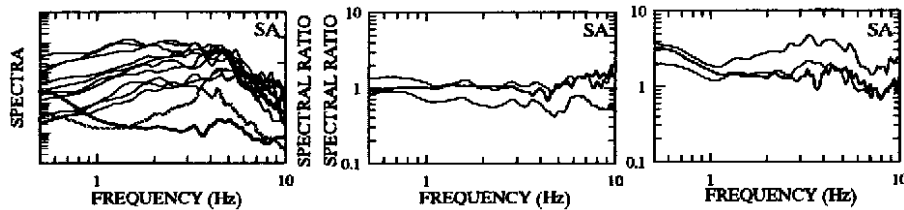


Figure 5. Compare microtremors and seismic motions on power spectra, HV and HH spectral ratios for HRKA-array.

3 CALCULATIONAL STUDY

3.1 Modeling and source mechanism

We examine the experimental conclusion by comparison numerical results in this chapter. We consider a two-dimensional surface wave and SV wave in a multi-layered medium by using the hybrid method of BEM and TLFEM [Fujiwara, 1996]. The wavefields are calculated in the model shown in Figure 6. As a example, modeling work is referenced the ground structure along north-south direction section in Kushiro district, because in this area remarkable spatial variation are observed. In Figure 6, domain $V(=\cup_{i=1}^N V^{(i)})$ is laterally heterogeneous and domains $V^{(A)}$ and $V^{(B)}$ are horizontally homogeneous layered media. The BEM in which the full-space Green's functions are adopted is used for application of V and the TLFEM is used for domains $V^{(A)}$ and $V^{(B)}$. The BEM can be combined with the TLFEM by matching the boundary conditions on the vertical boundaries $S^{(A)}(=\cup_{i=1}^N S_i^{(A)})$ and $S^{(B)}(=\cup_{i=1}^N S_i^{(B)})$. Relation equations between the displacement and the traction on boundaries $S^{(A)}$ and $S^{(B)}$ are required to match the boundary conditions. For domain $V(=\cup_{i=1}^N V^{(i)})$, the relation equations between the displacement and the traction are obtained directly from the formulation of the BEM. The most advantage of this method is to calculating properly surface wave wavefield such Love wave in SH-wavefield and Rayleigh wave in the P-SV-wavefield. The range of $V(=\cup_{i=1}^N V^{(i)})$ from vertical boundary $S^{(A)}$ and $S^{(B)}$ is 500m, and the maximum depth H is 3750m. The physics parameters of ground such P- and S-wave velocities, densities, and quality factors for each domain shown in the table 1. The parameters of $V^{(A)}$ and $V^{(B)}$ are same with those in adjoining part of $V(=\cup_{i=1}^N V^{(i)})$. The grid space of 2m and 4m-20m at free surface and the vertical boundary $V^{(A)}$ and $V^{(B)}$, respectively. Time step of 0.01 sec is used in the calculations.

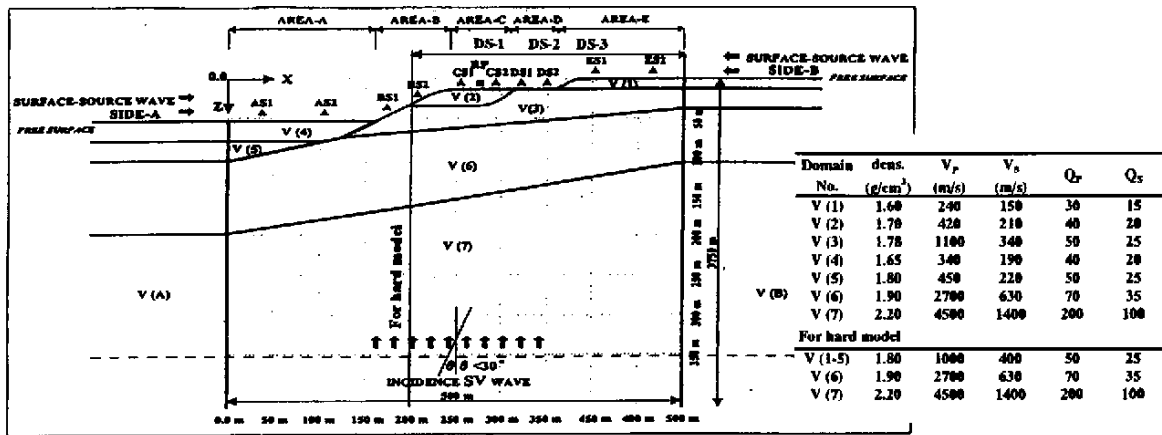


Figure 6. 2D laterally heterogeneous multi-layered sediment model.

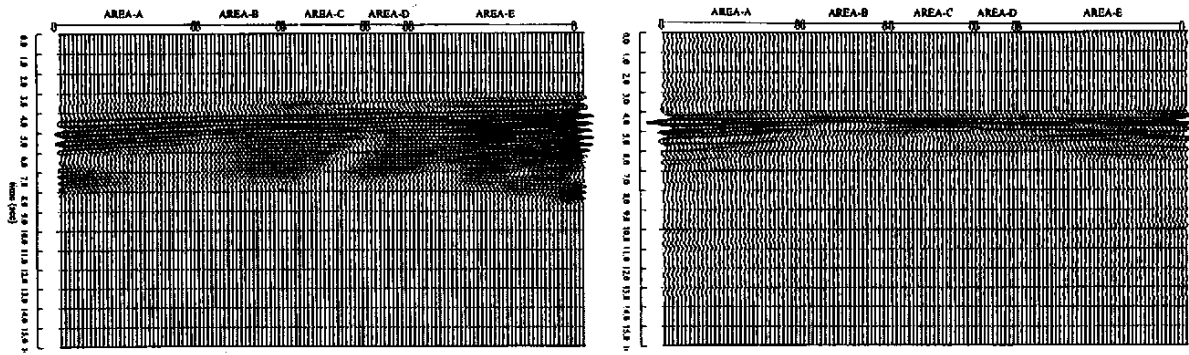


Figure 7. Horizontal waveforms due to horizontal surface source force (left diagram) and seismic SV wave incidence (right diagram).

We calculate seismic motions on a free surface produced by the incidences of plane SV wave. Incident angle is within 30° with. Microtremors are simulated by point source distributed on the free surface *SIDE-A* and *SIDE-B* of domain $V^{(A)}$ and $V^{(B)}$, respectively. The unit source force apply at horizontal direction and vertical direction. The strengths for both direction are assumed as similar because of we unknown the mechanism of natural sources as yet. The seismic motions and surface wave are synthesized with the frequency response up to 12.5Hz. We here consider frequency range from 0.5 to 10Hz in order to agree these of experimental result. The input motion $W(t)$ is Ricker wavelet and Butter worth wavelet. In this study, we name the synthesis waves for surface source waves to distinguish natural microtremors. We first show the examples of synthetic displacement waveforms (X-comp.) for the cases of the source apply horizontally on *SIDE-B* (+1200m, 0) in Figure 7 (left). The waveforms of *AREA-A*, *-B*, *-C*, *-D*, *-E* correspond to the areas at model (see Figure 6). We found that the waveforms show heavy spatial variation produced by the surface ground structures, though depth structures in this model are almost same, and mass surface waves are confirmed for contributed in the heterogeneous area. Figure 7 (right) show the examples of synthetic displacement waveforms (X-comp.) on the ground surface by plane SV wave incident. We found that similar patterns of spatial variation in both waveform are verified.

3.2 Stability and accuracy of surface source waves

To verify stability and accuracy of surface source wave, we calculated for the following two cases to examine whether the power spectra, HH and HV spectral ratios of surface source wave are dependent on sites than source spectra and structure of propagation path certainly or not, (a) changing the source force tensor direction as source effect, (b) changing the source location on both sides of the irregular structure as propagation path effect. As an example, the results of two cases shown in Figure 8. The reference site for HH ratio is site PR. For the case (a) in which the source force apply in X- (thin line) and Z-direction (thick line) simultaneously, clearly both HH and HV ratios are similar with two force direction whereas they are changing across 0.5-10Hz. However, the power-spectra is not same in low frequency range particularly. For the case (b) in which the source force apply on *SIDE-A* (thin line) and *SIDE-B* (thick line) simultaneously, both HH and HV spectral ratios show similar

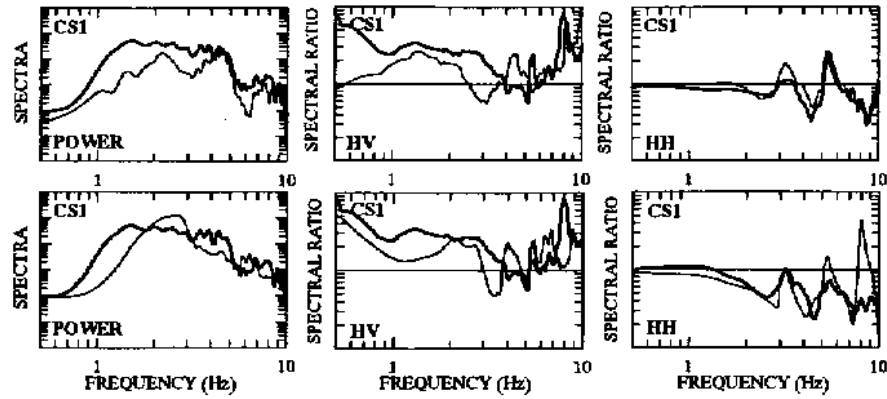


Figure 8. Effects of the propagation path (first row) and force directions (second row) of surface source waves on power spectra, HV and HH spectral ratios.

exclude power spectra too. These results shown that the power spectra are depended strongly by source and propagation path than on sites. Namely, the peak frequencies do not always coincide with predominant frequencies of ground. On the other hand, the HV spectral ratios are more effective than power spectra at exclusion of source effect and path effect. Again, the HH spectral ratios are stable and do not effect by source and path. Therefore, we compare the HV spectral ratios of surface source waves with power spectra of ground motions, HH and HV spectral ratios of surface source waves with those of seismic ground motions in the following.

3.3 Results of simulation analyses

Figure 9 show the results of comparison among surface source wave (thick line) and seismic motions (thin line). First row show the example of comparison results of amplification characteristics among HV spectral ratios of surface source waves and seismic SV waves spectra. The two thin lines represent results occurred by force apply on X- and Z- direction at the *SIDE-A*. The site locations are shown as triangle in Figure 6. We found that peak frequency of surface source waves showing clear peak existing at about 1.5Hz and these are coincide with those of seismic motions in all site exactly. However, they are different at high frequency range. The same results are obtained in which the sources apply on X- and Z- direction at the *SIDE-B*. These results correspond to those for experimental study with characteristics of predominant frequency.

Second row show the example of results of HH spectral ratios. The spectral ratios of surface source waves are the average generated by the force apply on X- and Z- direction at the *SIDE-A*. We found that both ratios are similar in all frequency range whereas they are changing from site to site. The same results are obtained in which the sources apply on X- and Z- direction at the *SIDE-B*. However, we also found that the correlation between both ratios became worse where both ground structure are fairly different (e.g. compare *AREA-A* and *AREA-C*). These results correspond to those for experimental study with characteristics of HH spectral ratios.

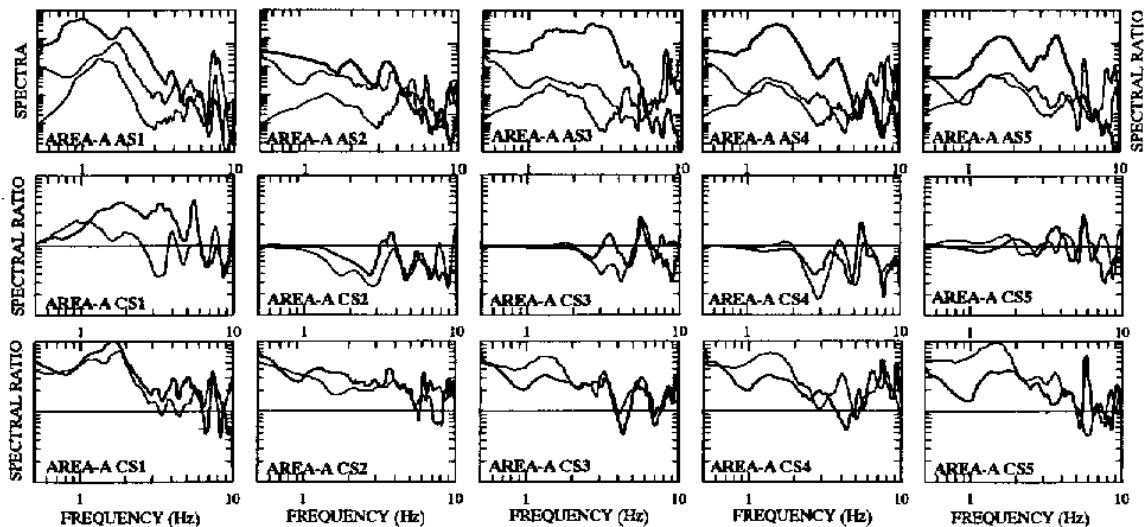


Figure 9. Amplification characteristics, HH and HV spectral ratios among surface source waves and seismic SV waves, the surface source waves ratios generated by horizontal force .

Bottom row show the example of comparison results of HV spectral ratios. In this case, the incident angle is 30° . The spectral ratios of surface source waves are the average occurred by force apply on X- and Z- direction at the *SIDE-A*. The both ratios are similar in 2.0-10Hz. The same results are obtained in which the sources apply on X- and Z- direction at the *SIDE-B*. These results correspond to those for experimental study with characteristics of HV spectral ratios.

3.4 Calculation results of hard surface ground model

To examine the results from the sites located on the diluvial deposits such HRKA-array, we simulate both characteristics using a multi-layered medium with hard surface ground. The model structure and physics parameters shown in Figure 6. The range of $V(=\cup_{i=1}^N V^{(i)})$ from vertical boundary $S^{(A)H}$ and $S^{(B)H}$ is 300m. The calculation conditions are same whit section 3.1. Figure 10 (left) show the examples of synthetic displacement waveforms (X-comp.) for the cases of source apply horizontally on *SIDE-B* (+1000m, 0), and Figure 10 (right) show the examples of synthetic displacement waveforms (X-comp.) on the ground surface by plane SV wave incident. We found that both waveforms show little for spatial variation. For stability and accuracy of surface source waves, we obtained different results with section 3.2 shown in Figure 11.

The power spectra is stable than the HV spectral ratios, and the peak is similar with the peak from ground motions shown in Figure12. For HV, HH spectral ratios, if the case which in horizontal direction force only, the characteristics show stable do not effect by the source and propagation path. We compare these HV, HH spectral ratios of surface source waves with those from ground motions (see Figure 13), and found that they almost similar. The results by comparison power spectra are correspond to those for HRKA-array, and the results by comparison HV, HH spectral ratios are correspond to results for HRKA-array only if the case which the force apply along horizontal direction.

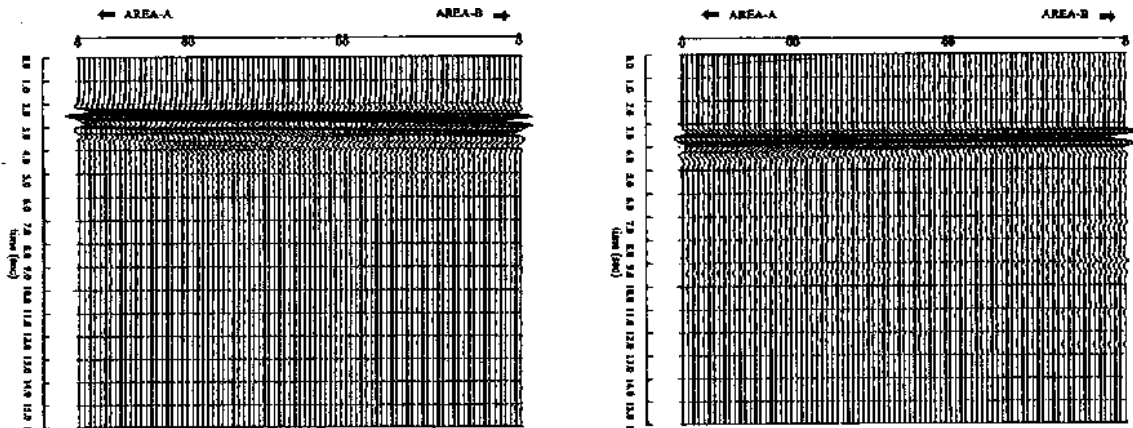


Figure 10. Horizontal waveforms due to horizontal surface source force (left diagram) and seismic SV wave incidence (right diagram) for hard surface ground model.

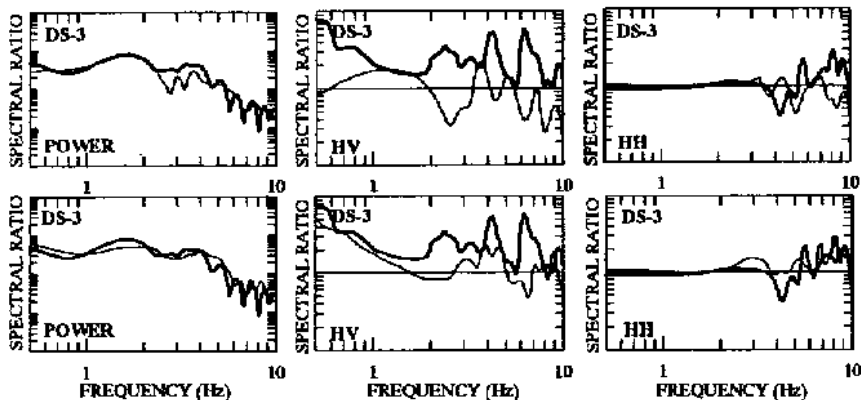


Figure 11. Effects of propagation path (first row) and force directions (second row) of surface source waves on power spectra, HV and HH spectral ratios for the hard model.

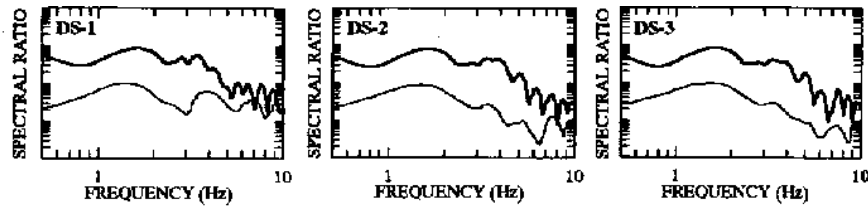


Figure 12. Amplification characteristics among surface source waves and seismic SV waves.

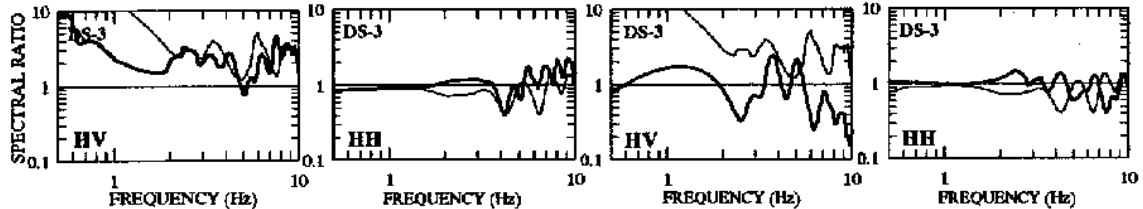


Figure 13. Left two diagrams show HV and HH spectral ratios among seismic SV waves and surface source waves generated by horizontal force and right two show those generated by vertical force.

4 CONCLUSION

In this study, we examined the reliability of seismic site-specific characteristics estimated from microtremor measurements by the experimentally and numerical studies. The following conclusions are obtained:

(1) The sharp-peak frequency of HV ratios is identified with the predominant frequency of seismic motion with high possibility, while a sharp-peak frequency of power spectra is not always identified with it. From this conclusion, it mentioned that the use of HV ratios are superior in the estimation of the predominant frequency on soft surface ground.

(2) The HH ratios inferred from microtremors show better agreement with those from seismic motion except high frequency range in respect to the smaller arrays.

This conclusion means that the spatial variation of seismic motion can be estimated from microtremor measurements as to the area where the microtremor source characteristics are supposed to be spatial uniform.

(3) The HV ratios of microtremors almost coincide with those of seismic motions.

This conclusion means the HV ratio can be utilized as transfer characteristics to predict vertical seismic motion from horizontal one.

ACKNOWLEDGMENTS

We think Prof. Horoshi Kawase, and Dr. Hiroyoki Fujiwara for great assistance. This research project is partially supported by the Grant-in-Aid for Developmental Scientific Research of the Japanese Ministry of Education, Science, Sports and Culture (No.05558047 and No.08248107).

REFERENCES

- Fujiwara, H. (1996), "Seismic Wavefields in Multi-Layered Media Calculated by Hybrid Combination of Boundary Element Method and Thin-Layer Finite Element Method, -The Case of Two-Dimensional P-SV-Wavefields", *J. Phys. Earth*, 44, 133-152.
- Irikura, K. and Kawanaka, T. (1980), "Characteristics of microtremors on ground with discontinuous underground structure", *Bull. Disast. Prev. Res. Inst., Kyoto Univ.*, 30-3, 81-96.
- Kanai, K., Osada, T. and Tanaka, T. (1954), "Measurement of the microtremors", *Bull. Earthq. Res. Inst. Tokyo Univ.*, 32, 199-209.
- Kanai, K. (1957), "The requisite condition for the predominant vibration of ground", *Bull. Earthq. Res. Inst.*, 35, 457-471.
- Zhao, B. M., Horike, M. and Takeuchi, Y. (1996), "Comparison of spatial variation between microtremors and seismic motion", *Proc. 11th World Conf. Earthq. Eng.*, Paper No.133.
- Zhao, B. M., Horike, M., Takeuchi, Y. and Kawase, H. (1997), "Comparison of site-specific response characteristics inferred from seismic motions and microtremors", *Journal of seism. Soc. Japan (ZISIN)*, 2, 50, 67-87 (in Japanese).
- Zhao, B. M., Horike, M. and Takeuchi, Y. (1998a), "Which site-specific characteristics estimated from microtremors are useful?", *Journal of Struct. Constr. Eng. Japan (AIJ)*, 509, 69-75 (in Japanese).
- Zhao, B. M., Horike, M. and Takeuchi, Y. (1998b), "Reliability of estimation of seismic ground characteristic by microtremor observation", *Proc. 11th European Conf. Earthq. Eng.*